Physicochem. Probl. Miner. Process., 58(1), 2022, 37-49

http://www.journalssystem.com/ppmp

Physicochemical Problems of Mineral Processing

ISSN 1643-1049

Received August 26, 2021; reviewed; accepted November 12, 2021

Application of uniform test design in optimizing the flotation reagents of iron anionic reverse flotation circuit

Ying Hou [1], Ahmed Sobhy [2,3]

[1] School of Mining Engineering, University of Science and Technology Liaoning, Anshan 114051, China

[2] School of Resources and Environmental Engineering, Shandong University of Technology, Zibo, 255049, China

[3] Minerals Technology Department, Central Metallurgical R&D Institute, Helwan, Cairo, 11421, Egypt

Corresponding author: asobhy81@gmail.com (Ahmed Sobhy)

Abstract: Most iron reserves are low in grade with quartz as the main gangue mineral, and anionic reverse flotation has become the most crucial separation method in the processing plants of iron ore. Thus, a flotation feed sample that is a mixture of low-intensity and high-gradient magnetic separators concentrates was acquired from a processing plant. The sample characterizations with X-ray diffraction (XRD), X-ray fluorescence (XRF), laser particle size analyzer, and mineral liberation analysis (MLA) confirmed that the sample consists of iron oxide as a valuable mineral and quartz as a gangue mineral with adequate liberation degree. In the anionic reverse flotation, the interaction of the flotation reagents with the constituents of the feed makes the flotation a complex system. Thus, the selection and optimization of regent dosages were performed using a uniform experimental design to estimate the optimum separation efficiency. The optimum reagent system was 1.6 kg/Mg starch depressant, 1.0 kg/Mg calcium oxide (lime) activator, and 0.8 kg/Mg TD-II anionic collector. At the optimum, 68.90% iron grade with 92.62% recovery was produced.

Keywords: iron oxide, quartz, uniform test design, reverse flotation, optimization, flotation reagents

1. Introduction

Iron ores are scattered in all parts of China with verified ore reserves of about 80 billion tons, but most reserves are low in grade with an average grade of 30.5% total iron (Li et al., 2015; Tang et al., 2019). 1.70 billion tons of these proven reserves are located in the Southern Anshan area in Liaoning Province, which is equivalent to reserves of 0.68 billion tons with an average grade of 34% total iron (Li et al., 2015).

With a cut-off grade of 45% total iron, the iron ore resources are diminishing. Thus the iron and steel industries seek beneficiation of low grade (below 45%) iron ore resources to meet the demand. For the effective utilization of iron ore resources, research efforts have been directed towards technology development for the beneficiation of low-grade iron ore (Zhang et al., 2019; Pattanaik and Venugopal, 2018; Nakhaei and Irannajad, 2017). For example, researchers have designed the processing plant of Anshan Iron and Steel Company (Chen and Xiong, 2015) that consists of several stages such as grinding, coarse classification, coarse particles gravity separation, fine particles low and high-intensity magnetic separation, and anion reverse flotation process, which is utilized by many large and medium-sized domestic mining companies (Chen and Xiong, 2015). Furthermore, the flowsheet of processing iron ore in Anshan Iron and Steel Company is now widely applied over the world, for the primary concentration of iron ore (Chen and Xiong, 2015).

The floatability phenomenon of iron ores varies extensively, due to the differences in the chemical and physicochemical properties in terms of iron minerals and the nature of accompanied gangue minerals, which results in the diverse flotation routes (Montes and Montes-Atenas, 2005). Generally, the common gangue minerals associated with iron ore are silica, alumina, sulfur, and phosphorous in

DOI: 10.37190/ppmp/143889

different chemical forms (Pattanaik and Venugopal, 2018). To make a specific mineral float, the surface of such a mineral has to be adapted by the adsorption of appropriate surfactants. Thus, the reagents should be selected effectively for the accomplishment of good separation performance of minerals. Furthermore, maximizing the floatability of chosen minerals with the assistance of reagents is the key to an effective and efficient flotation process.

For iron ore reverse flotation in which gangue minerals such as quartz are floated while the iron minerals remain depressed in the slurry, the reagent system involves pH regulators, depressants, activators, and collectors. The reverse cationic flotation is not preferable due to the high cost of amine collectors in addition to the foam problem as well as the metal loss at the de-sliming stage required in cationic reverse flotation (Ma et al., 2011), thus anionic reverse flotation is the common route.

Reverse anionic flotation is carried out at a high pH value of 11–12 adjusted by a pH modifier such as sodium hydroxide (Ma et al., 2011). Thus, the repulsive electrostatic forces between the negatively charged quartz and iron oxide particles are very strong, before the addition of iron oxide depressants such as corn starch. Then calcium oxide (lime) selectively activate quartz particles by varying its surface positive to allow the anionic collector adsorption (Ye and Matsuoka, 1993). Besides, too much lime could be destructive for reverse anionic flotation as a result of calcium ion adsorption on the ultra-fine iron oxide particles and in consequence the adsorption of the anionic collector in addition to the adsorption of calcium ion with hydroxide ion on quartz particles hindering the flotation performance (Pattanaik and Venugopal, 2018; Yang et al., 2013).

In summary, a satisfactory flotation performance in the processing plant with a suitable reagent system is a critical process, especially when dealing with complex and difficult-to-upgrade iron ores. Besides, froth flotation has become the most crucial separation technique in the processing of medium-grade and low-grade iron ores (Quast, 2017; de-Medeiros and Baltar, 2018; Kumar et al., 2018; Yin et al., 2019).

The interaction of the flotation reagents with the various constituents of the ore in the slurry makes the flotation a difficult system (Chander and Nagaraj, 2007). Furthermore, the regent selection and optimization based on the reagent-mineral interactions is a critical analysis step, thus a uniform experimental design can be used which has the characteristics of "uniform scattering, tidy and comparable". It is a highly efficient, fast, and economical experimental design method that reduces test times, shortens test cycles, and finds multi-factor optimization schemes quickly (Wang et al., 2001; Xia et al., 2016). Many researchers have applied the uniform test design to study the best reagent system for iron oxide reverse flotation and for flotation processes of other minerals (Guo et al., 2011; Gao et al., 2013; Lubisi et al., 2018; Pattanaik and Rayasam, 2018). For example, Gao et al. (2013) estimated the optimum anionic reverse flotation of iron oxide magnetic separation products using a uniform design to be 63.83% grade and 84.59 recovery at the optimum conditions of 1.00 kg/t depressant, 2.00 kg/t activator, and 1.28 kg/t collector dosages. In addition, Wang et al. (2019) showed that the absence of activator reduced extremely the flotability of quartz by about 90%. Besides, Shrimali et al. (2018) found that excessive depressant dosage not only depress iron oxide but also depressed quartz. Thus, it is vital to employ uniform design to find the best suitable reagent system for iron anionic reverse flotation circuit faster and efficiently.

In this paper, the flotation experiments of the mixed magnetic separation concentrates of the Anqian processing plant were carried out using the uniform test design method to investigate and optimize the influences of the flotation reagents.

2. Materials and methods

2.1. Materials

The experimental sample was acquired from the Anqian processing plant located in Anshan, Liaoning, China. The sample is a mixture of two concentrates from low-intensity magnetic and high-gradient magnetic separations as shown in Fig. 1 to be upgraded in a reverse flotation circuit.

Fig. 1 is the iron processing flowsheet, which indicates that the ore is crushed, ground, and screened into fine and coarse fractions. The coarse fraction is fed into spirals to produce a high-grade iron concentrate, and its tailings are successively processed by low-intensity magnetic and high-gradient magnetic separations, with a relatively high-grade concentrate achieved and returned to the grinding-

classification system to achieve full liberation. The fine fraction is processed with low-intensity magnetic separation to achieve a magnetite concentrate, and its tailings are processed with SLon pulsating high-gradient magnetic separators to achieve a hematite concentrate. These two concentrates are combined and upgraded in a reverse flotation flowsheet to produce a high-grade concentrate. This concentrate is combined with that from the coarse fraction and produces a final concentrate at a high recovery value (Chen and Xiong, 2015). The as-received samples at the lab were dried, mixed, split into smaller portions, and sealed for later usage.

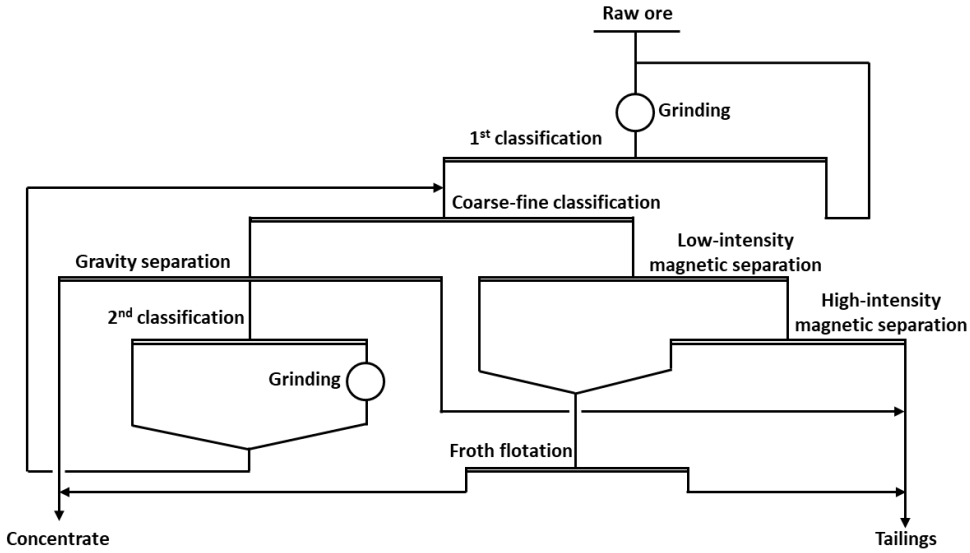

Fig. 1. Iron oxide processing flowsheet

2.2. Sample characterization

Representative samples were characterized using X-ray diffraction (XRD), X-ray fluorescence (XRF), laser particle size analyzer, and mineral liberation analysis (MLA). XRD analysis was used to identify the mineral combination of the flotation feed sample. Also, XRF analysis was conducted to confirm that the main constituents of the tested sample. In addition, laser particle size analysis was used to measure the particle size distribution. Besides, mineral liberation analyzer MLA 650F (FEI, USA) was applied for quantitative mineralogical characterization of the flotation feed sample and to identify the degree of liberation between valuable and gangue minerals.

As seen from Fig. 2, XRD spectrum, the sample consists of hematite and magnetite as a valuable minerals and quartz as a gangue mineral. Besides, the XRF analysis shown in Table 1 confirms that the main constituents of the experimental sample are 48.13% Fe_2O_3 and 50.28% SiO_2 in addition to small percentages of other impurities such as P and S.

The size distribution of the representative sample shown in Fig. 3 was estimated by conducting a laser particle size analyzer (BT-9300S) made by Bettersize Instrument Ltd., Dandong, China. It shows that 90% of the sample is finer than 104 microns.

Furthermore, quantitative mineralogical characterization of the mixed magnetic separation concentrates (flotation sample) was performed with a mineral liberation analyzer MLA 650F (FEI, USA). MLA given in Table 2 shows that 90% and 67% of iron oxide and quartz particles respectively are liberated with a purity of more than 90%. Whereas, the other harmful elements for the steel industry such as sulfur and phosphorous are not free, but their grades are very small in an acceptable range. More details were illustrated about the sample characteristics were presented in a previous work (Tao et al., 2021; Sobhy et al., 2021).

Table 1. X-ray fluorescence analysis of the representative sample

Fe_2O_3	Na_2O	MgO	Al_2O_3	SiO_2	K_2O	CaO	P	S	Cu	Pb	Zn	Co	BaO
48.1335	0.0368	0.5973	0.1065	50.2756	0.0192	0.5296	0.0934	0.1082	0.0146	0.03	0.016	0.0016	0.1377

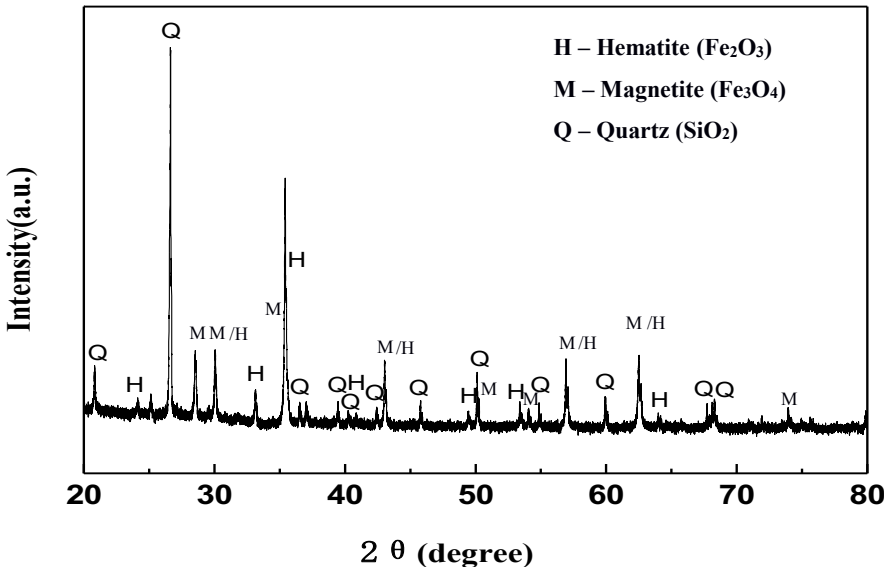

Fig. 2. X-ray diffraction analysis spectrum of the representative sample

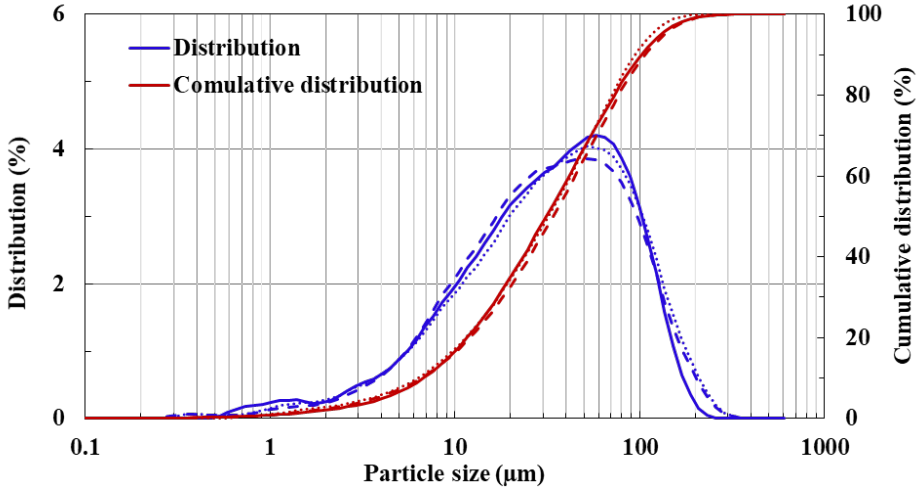

Fig. 3. Laser particle size analysis of the representative sample

Table 2. MLA liberation degree analysis of main minerals in the representative sample

Locked condition	0-30% locked	30-60% locked	60-90% locked	Liberated Particles (%)
Iron oxide	1.49	2.3	6.01	90.19
Quartz	3.82	6.73	21.73	67.72
Pyrite	14.63	7.35	30.18	47.85
Apatite	26.78	12.43	14.66	46.14

2.3. Technical and operational flotation conditions

The action mechanism of the flotation reagent consists of four different kinds of reagents performing diverse influences during the anionic reverse flotation. Sodium hydroxide (NaOH) adjusts the pulp pH value to change the surface potential of the minerals to exert an effect on the status of the other reagents. Under the alkaline conditions, starch depresses mainly floating iron oxide particles (Yin et al., 2019, Ravishankar and Khosla, 1995; Weisseborn et al., 1995; Filippov et al., 2010; Luo et al., 2016; Yin et al., 2016, 2017). Calcium oxide (CaO) is utilized to strongly activate quartz at a pH value higher than 11 since CaO is dissolved to form calcium hydroxide ($Ca(OH)_2$) to produce $Ca(OH)^+$. Furthermore, when

the pH is lower than 11, the amount of H^+ is relatively high, and CaO presents in the water mostly in the form of Ca^{2+} causing a weak activation. The effect of an anionic collector, TD-II, is to collect quartz that is activated by $Ca(OH)^+$.

The reverse flotation experiments of iron oxide were carried out by using XFD-III 1.5L temperature-controlled flotation machine according to the closed-circuit shown in Fig. 4. Unless otherwise specified, the experiments were done under the following processing plant conditions: pH 11.5, temperature 30^o C, solids percentage 33.3% by weight, starch and lime conditioning time 3 min each, TD-II collector conditioning time 2 min, rotor speed of flotation machine 1500 rpm, and flotation time 3 min. Flotation concentrate and tailings were assayed for total iron (Fe) content to determine performance parameters such as yield, Fe grade, Fe recovery, and separation efficiency. Determination of the total Fe grade was carried out by using the most widely used titrimetric method with standard solution of potassium dichromate (Knop, 1924).

Flotation reagents shown in Table 3 are commercial products obtained from the Anqian processing plant and were used as is in the reverse flotation of iron oxide (Sobhy el al. 2021, Tao et al., 2020). Sodium hydroxide is the pH modifier, starch + K6-1 is the iron oxide depressant, calcium oxide is the quartz activator, and TD-II is the quartz anionic collector.

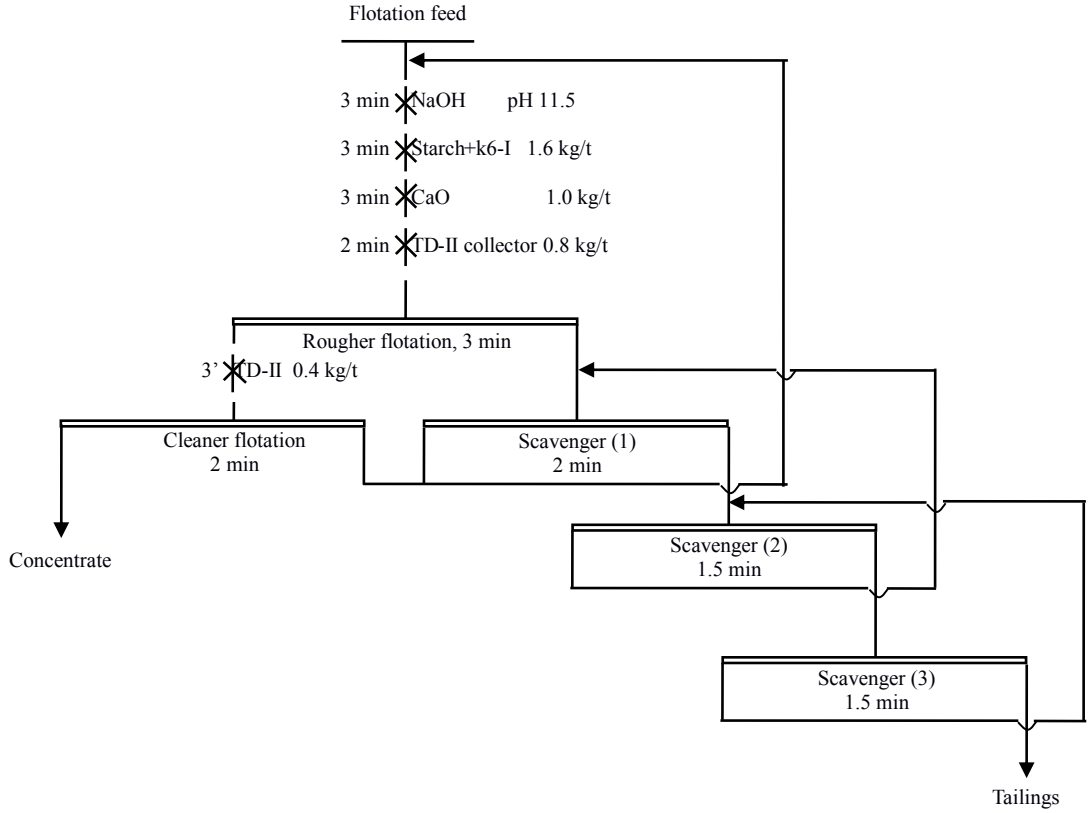

Fig. 4. The closed-circuit reagent system and process flow chart of one rough, one fine, and three-scavenger flotation units

Table 3. Details of chemical reagents used in the reverse flotation of iron oxide

Reagent	Role	Chemical formula	specification	Manufacturer
Sodium hydroxide	pH modifier	NaOH	Analyze pure AR	Shanghai Aladdin Biochemical Technology Co., Ltd.
Starch + K6-1	Depressant	$(C_6H_{10}O_5)_n$	Commercial products	Angang Group Anqian Mining Co., Ltd.
Calcium Oxide	Activator	CaO	Analyze pure AR	Shanghai Aladdin Biochemical Technology Co., Ltd.
TD-II	Collector	-	Commercial products	Angang Group Anqian Mining Co., Ltd.

Generally, the grade of concentrate recovered from a single stage of flotation is not high enough and requires re-floating in one or more stages of flotation referred to as cleaner or recleaner stages. The series of cells that produce the initial concentrate is called the rougher stage and any subsequent retreatment of the rougher tailings is referred to as scavenging (Gupta, Yan, 2016).

2.4. Uniform experimental design

The uniform design of iron reverse flotation experiments using MATLAB 7.1 was conducted to find the best setup enhancing the separation efficiency. Computer simulation is performed to simulate the process behavior and to obtain an approximate model presenting the actual process performance as shown in Fig. 5. Due to the complexity of the reverse flotation system, special experimental design is required such as a uniform design. The uniform design is usually employed in many industrial experiments.

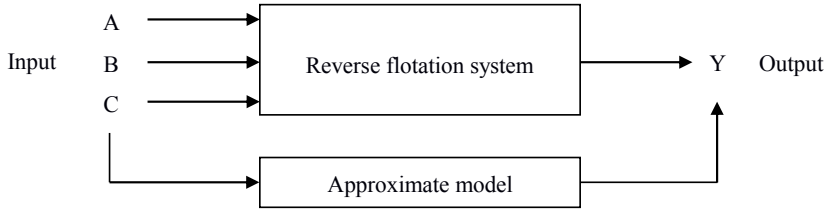

Fig. 5. Computer simulation of experiments

Uniform designs are tabulated with a representation of $U_n(q^S)$, where U, n, q, s stand for uniform design, number of runs, number of levels, and for number of factors, respectively (Zhang et al., 2018). In this case, there are three factors including depressant dosage (A), activator dosage (B), and collector dosage (C). Whereas, the separation efficiency (Y) is the response variable. Thus, the uniform experimental design $U_{10}(10^3)$ which stands for 10-run of uniform design for 10-level of 3 factors as shown in Table 4 was used to find the best dosage of flotation reagents, and evenly distribute the dosage of each factor within the appropriate dosage range.

The appropriate experimental domain was determined through the preliminary experiments to be [0.4, 2.2] x [0.1, 1.0] x [0.3, 1.2], and each factor takes 10 levels in this domain as shown in Table 4 where the 10 levels marked by 1, 2, …… 10 are changed into the true levels of the factors (Table 5). Then the experiments are run in a randomized order besides duplicating one of the experiments with taking the average values, and the response variable is estimated, the best result among the 10 responses is taken as the benchmark, and the level-combination may produce a better response. Furthermore, the most advantage of the uniform design is to generate a suitable model, which could be a simple first-order model or a more complicated second-order centered quadratic model.

The obtained test results specifically the separation efficiency shall be used for data processing and analysis of variance by SPSS to establish suitable models fitting the data. Then, statistical diagnostics are performed to check the acceptability of the predicted model.

Table 4. U_{10} (10^3) uniform test design of iron reverse flotation

Run	Inhibitor (A)	Activator (B)	Collector (C)
1	1	5	7
2	2	10	3
3	3	4	10
4	4	9	6
5	5	3	2
6	6	8	9
7	7	2	5
8	8	7	1
9	9	1	8
10	10	6	4

Table 5. The experimental domain for each factor with 10 levels for iron reverse flotation

Run	Depressant (A) (kg/Mg)	Activator (B) (kg/Mg)	Collector (C) (kg/Mg)
1	0.4	0.5	0.9
2	0.6	1.0	0.5
3	0.8	0.4	1.2
4	1.0	0.9	0.8
5	1.2	0.3	0.4
6	1.4	0.8	1.1
7	1.6	0.2	0.7
8	1.8	0.7	0.3
9	2.0	0.1	1.0
10	2.2	0.6	0.6

The separation efficiency of the circuit of iron reverse flotation, which is considered a typical two-component separation process is usually estimated by formulas such as Hancock's formula, Fleming's formula, and Doulas' formula (Zhang et al., 2018; Hou et al., 2021). From the built model, the best combination of the factors values of the optimum reagent system that maximizes the separation efficiency values was determined.

3. Results and discussion

3.1. Closed-circuit flotation flow-sheet

The closed-circuit shown previously in Fig. 4 has been conducted based on the typical plant conditions which consuming 1.2 kg/Mg depressant, 0.5 kg/Mg activator, and 0.8 kg/Mg collector in the rougher stage in addition to 0.4 kg/Mg collector in the cleaner stage to beneficiate a flotation feed with a grade of about 48% total iron. The results shown in Table 6 demonstrate that iron concentrate with 68.28% total Fe grade and 89.07% Fe recovery has been produced.

Table 6. Closed-circuit flotation results at a flotation

Product name	Yield/%	Fe grade/%	Fe recovery/%
Concentrate	62.49	68.28	89.07
Tailings	37.51	13.95	10.93
Experimental feed	100.00	47.90	100.00

Due to the complexity of the technological parameters and operational conditions, a uniform experimental design has been utilized as illustrated in the next section to investigate the interaction between the independent variables and to find the optimum performance.

3.2. Uniform experimental design

Anionic reverse flotation tests with iron oxide feed samples were systemically performed according to the test schemes shown in Table 4 and Table 5 using the flotation separation flowchart given in Fig. 4, and the obtained test results are shown in Table 6. Data analysis using SPSS software is shown in Table 7. It can be seen from Table 6 that the best factor values are 0.6 kg/Mg depressant dosage, 1.0 kg/Mg activator dosage, and 0.5 kg/Mg collector dosage which produced the highest separation efficiency of 68.65%. Using this test condition which is beneficial for the separation of quartz from iron oxide has given 58.93% yield with 66.32% Fe grade and 82.14% Fe recovery. This could be used as a benchmark, and the uniform design is utilized to know whether there is any level-combination producing a higher separation efficiency.

The separation efficiency model evaluates how the response is connected to the independent factors and their interactions. Thus, as an output projected by the uniform experimental design, the final empirical models of coded factors for separation efficiency is shown below:

Table 6. Uniform test design results of reverse flotation separation of the iron oxide sample with variable reagents

Test No.	Dosage of reagent (kg/Mg)		Product	Yield (%)	Fe grade (%)	Fe recovery (%)	Separation efficiency (%)
	A :	0.4	Concentrates	47.63	66.88	67.74	
1	B :	0.5	Tailings	52.37	28.97	32.26	58.54
	C :	0.9	Feed	100.00	47.03	100.00	
	A :	0.6	Concentrates	58.93	66.32	82.14	
2	B :	1	Tailings	41.07	20.70	17.86	68.65
	C :	0.5	Feed	100.00	47.59	100.00	
	A :	0.8	Concentrates	53.23	64.17	71.31	
3	B :	0.4	Tailings	46.77	29.39	28.69	52.49
	C :	1.2	Feed	100.00	47.90	100.00	
	A :	1	Concentrate	66.67	64.75	88.47	
4	B :	0.9	Tailings	33.33	16.87	11.53	66.57
	C :	0.8	Feed	100.00	48.79	100.00	
	A :	1.2	Concentrates	67.21	62.05	86.14	
5	B :	0.3	Tailings	32.79	20.47	13.86	54.41
	C :	0.4	Feed	100.00	48.42	100.00	
	A :	1.4	Concentrates	65.12	61.75	81.97	
6	B :	0.8	Tailings	34.88	25.36	18.03	49.68
	C :	1.1	Feed	100.00	49.06	100.00	
	A :	1.6	Concentrate	63.46	61.79	81.74	
7	B :	0.2	Tailings	36.54	23.98	18.26	51.27
	C :	0.7	Feed	100.00	47.98	100.00	
	A :	1.8	Concentrate	74.37	56.11	85.45	
8	B :	0.7	Tailings	25.63	27.72	14.55	29.37
	C :	0.3	Feed	100.00	48.83	100.00	
	A :	2	Concentrates	56.35	61.21	71.85	
9	B :	0.1	Tailings	43.65	30.96	28.15	43.13
	C :	1	Feed	100.00	48.01	100.00	
	A :	2.2	Concentrate	67.19	53.98	75.69	
10	B :	0.6	Tailings	32.81	35.51	24.31	20.77
	C :	0.6	Feed	100.00	47.92	100.00	

$$\text{Separation efficiency} = 56.610 - 4.791A + 27.143C + 9.361A^2 - 11.196B^2 - 32.369A^2B + 39.579B^2A - - 12.312\ C^2A - 64.851C^2B + 61.696ABC \quad (1)$$

with R^2 and adjust R^2 close to unit value and negligible standard error, where the positive sign indicates the synergistic impacts and the negative sign shows the antagonistic influences. The model terms refer to depressant (A), collector (C), depressant's quadratic (A^2), activator's quadratic (B^2), the interaction of depressant's quadratic and activator (A^2B), the interaction of activator's quadratic and depressant (B^2A), the interaction of collector's quadratic and depressant (C^2A), the interaction of collector's quadratic and activator (C^2B), and the interaction of depressant with activator and collector (ABC). Whereas the separation efficiency (Y) is the dependent variable.

The comparison between the actual experimental values and the predicted values of response coefficients projected by the model (Table 7) confirms that the estimated response is agreeable with the

actual experimental data since the relative error is less than 0.01 signifying the accuracy of the established mathematical model.

Table 7. Predicted value, test value, and prediction error of the mathematical model

Test No.	Separation efficiency (%)	Predicted value of separation efficiency (%)	Error (%)
1	58.5400	58.5432	-0.0024
2	68.6500	68.6547	-0.0039
3	52.4900	52.4908	0.0021
4	66.5700	66.5788	-0.0040
5	54.4100	54.4090	0.0003
6	49.6800	49.6798	-0.0008
7	51.2700	51.2687	-0.0002
8	29.3700	29.3798	-0.0065
9	43.1300	43.1331	0.0013
10	20.7700	20.7763	-0.0046

3.3. Factors combined effects and optimization

Response surface modeling (Khayet et al., 2008) has been used to explain and elucidate the interactions between every two variables influencing the separation efficiency while other variables are kept at their best values.

Fig. 6 shows the interaction effects of starch depressant dosage and lime activator dosage on the separation efficiency at the best value of the TD-II collector dosage (C: 0.8 kg/Mg). The minimum separation efficiency was obtained by increasing the activator dosage and decreasing the depressant dosage. Whereas the separation efficiency was enhanced by keeping the activator dosage at its high level of 1.0 kg/Mg and by increasing the depressant dosage to 1.6 kg/Mg. Usually, the activator is essential for the flotation of quartz (Sobhy et al., 2021), and a higher depressant dosage and consequently a higher adsorption density on the iron oxide surface is expected to have a stronger depression influence on iron oxide minerals (Yang, Wang, 2018). Furthermore, optimum separation efficiency has been given at 1.0 kg/Mg activator dosage and 1.6 kg/Mg depressant dosage (Fig. 6). The interaction between the activator and depressant dosages positively affected the separation efficiency. This is because the depressant and activator dosages significantly effectively depress the iron oxide particles and activate the quartz particles respectively for an efficient flotation process by the anionic collector at 11.5 pH value since the flotation technique relies on the enhanced capture of hydrophobic minerals by micro- bubbles, while the hydrophilic minerals settle down to the tailings stream (Laplante et al., 1993; Sobhy et al., 2019). Furthermore, the depressant dosage showed major influences on the separation efficiency in comparison with the activator dosage.

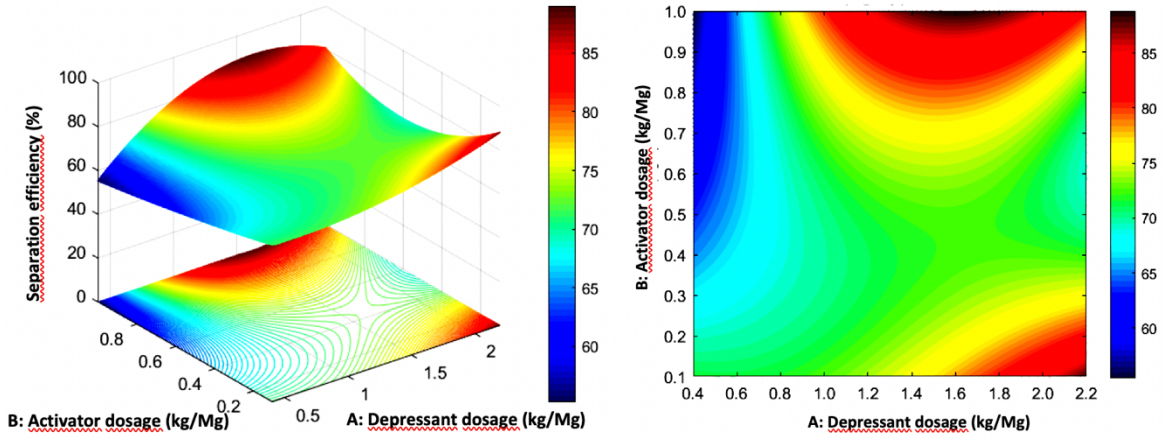

Fig. 6. Response surface and contour plots showing the interaction between depressant dosage (A) and activator dosage (B) affecting the flotation separation efficiency at 0.8 kg/Mg collector dosage (C)

Fig. 7 shows the interaction effects of depressant dosage (A) and collector dosage (C) on the separation efficiency at the best value of the activator dosage (B: 1.0 kg/Mg). The interaction of these two variables at the best condition of the third variable had a significant impact on the separation efficiency which reached its maximum value at 1.6 kg/Mg and 0.8 kg/Mg depressant and collector dosages respectively, and any deviation from these optimum values of the factors caused a significant decrease in the separation efficiency. This can be attributed to the high depressant dosage that enhances the recovery and reduces the concentrate grade, which results in decreasing the separation efficiency (Lima et al., 2013). Thus, the depressant dosage of 1.6 kg/Mg was necessary to depress iron oxide effectively without affecting the floatability of quartz particles. Besides, a higher collector dosage of more than 0.8 kg/Mg increases the concentrate grade and decreases the recovery, which negatively affects the separation efficiency.

Fig. 8 shows the interaction effects of activator dosage (B) and collector dosage (C) at the best value of the depressant dosage (A: 1.6 kg/Mg). The activator significantly influences the effect of the collection. Surprisingly, an increase in the activator dosage from 0.1 kg/Mg to 0.5 kg/Mg slightly reduced the separation efficiency by 5 to 10%, but the further increase in the activator dosage from 0.5 kg/Mg to 1.0 kg/Mg increased significantly the separation efficiency to reach its maximum value of 90% at 0.8 kg/Mg collector dosage. Furthermore, increasing the collector dosage from 0.3 kg/Mg to 0.8 kg/Mg increased the separation efficiency to reach maximum. Sobhy et al (2021) found that collector dosage above 0.5 kg/t with a lime dosage of about 0.7 kg/t was necessary to achieve iron grade above68%. The further increase in the collector dosage negatively affected the separation efficiency probably as a result of a co-adsorption by undepressed iron oxide particles.

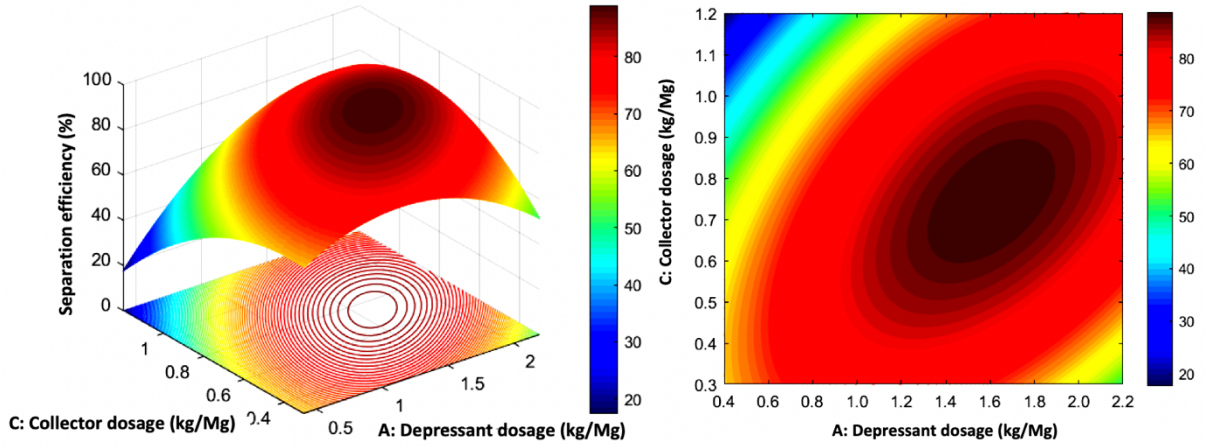

Fig. 7. Response surface and contour plots showing the interaction between depressant dosage (A) and collector dosage (C) affecting the flotation separation efficiency at 1.0 kg/Mg activator dosage (B)

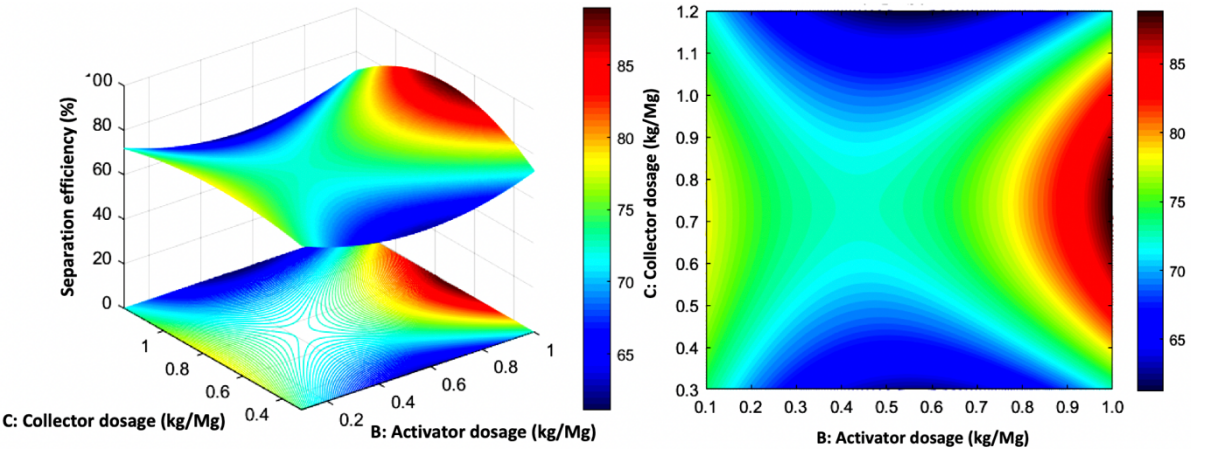

Fig. 8. Response surface and contour plots showing the interaction between activator dosage (B) and collector dosage (C) affecting the flotation separation efficiency at 1.6 kg/Mg depressant dosage (A)

The necessary part of the uniform experimental design was to predict the optimum reagent system where maximum separation efficiency (maximum Fe grade and recovery) can be produced. In the current study as shown in Table 8, the predicted maximum Fe grade and recovery of 68.90% and 92.62% respectively were obtained at optimum conditions of 1.6 kg/Mg depressant dosage, 1.0 kg/Mg activator dosage, and 0.8 kg/Mg collector dosage. The average grade and recovery from two verification experiments under the optimum conditions were 68.60% and 91.75%, respectively, which were approximately similar to the predicted values.

Table 8. Closed circuit optimum flotation results

Product	Yield (%)	Fe grade (%)	Fe recovery (%)
Concentrates	63.35	68.90	92.62
Tailings	36.65	9.49	7.38
Feed	100.00	47.12	100.00

4. Conclusions

A uniform experimental design has been conducted to evaluate and optimize the effects of three independent parameters in the reverse anionic iron oxide flotation process. The results show that starch depressant, calcium oxide activator, and TD-II anionic collector have a significant impact on product yield, iron grade, iron recovery, and separation efficiency. The optimum conditions to produce maximum iron grade and recovery have been determined to be 1.6 kg/Mg depressant, 1.0 kg/Mg activator, and 0.8 kg/Mg collector. Under these optimum values, the maximum recovery was 92.62% at a grade of 68.90%. Besides, the calculated response is agreeable with the actual experimental data indicating the accuracy of the established mathematical separation efficiency model.

Acknowledgments

The authors are grateful for the financial support provided to this research project by the Natural Science Foundation of Liaoning Province (No.20180550198), Department of Education of Liaoning Provincial (No. 2016TSPY12, 2019LNQN09), Science and Technology Plan of Anshan City (No. 110000144), Key R&D Program of Liaoning Province (No. 2017230002), Liaoning University of Science and Technology Youth Fund Project (No. 2015QN13), and Liaoning University of Science and Technology National Fund Preliminary Research Project (No. 2017YY05) which made this study possible.

References

CHANDER, S., NAGARAJ, D.R., 2007. *Flotation/ Flotation Reagents. Encyclopedia of Separation Science, Reference Module in Chemistry.* Molecul. Sci. and Chem. Eng. 1-14.

CHEN, L., XIANG, D., 2015. *Chapter seven - magnetic techniques for mineral processing*. in Progress in Filtration and Separ. 287-324.

DE MEDEIROS, A.R.S., BALTAR, C.A.M., 2018. *Importance of collector chain length in flotation of fine particles.* Miner. Eng. 122, 179–184.

FANG, K.T., LIN, D.K.J., 2003. *Ch. 4. Uniform experimental designs and their applications in industry.* Handbook of Statistics, Elsevier 22, 131-170.

FILIPPOV, L.O., FILIPPOV, I.V., SEVEROV, V.V., 2010. *The use of collectors mixture in the reverse cationic flotation of magnetite ore: the role of Fe-bearing silicates.* Miner. Eng. 23 (2), 91–98.

GAO, Y., ZHANG, Y.H., OUYANG, G.Z., 2013. *The Anionic Reverse Flotation Orthogonal Experiment for XuanLong Oolitic Hematite after Magnetic Roasting-Magnetic Separation.* Adv. Materials Research 826, 130–135.

GUO, C., WANG, H., FU, J.G., CHEN, K.D., 2011. *Recovery a Refractory Oolitic Hematite by Magnetization Roasting and Magnetic Separation.* Adv. Materials Research 361–363, 305–310.

GUPTA, A., YAN, D., 2016. *Flotation in Mineral Processing Design and Operations (Second Edition)*. ISBN: 978-0-444-63589-1

HOU, Y., SOBHY, A., WANG, Y., 2021. *Significance of reagents addition sequence on iron anionic reverse flotation and their adsorption characteristics using QCM-D.* Physicochem. Probl. Miner. Process., 57(1), 284-293.

KHAYET M., COJOCARU C, ZAKRZEWSKA-TRZNADEL G., 2008. *Response surface modeling and optimization in pervaporation.* J. Membrane Sci. 321(2), 272-283.

KNOP, J., 1924. D*iphenylamine as indicator in the titration of iron with dichromate solution.* J. Am. Chem. Soc., 46(2), 263–269.

KUMAR, D., JAIN, V., RAI, B., 2018. *Can carboxymethyl cellulose be used as a selective flocculant for beneficiating alumina-rich iron ore slimes? A density functional theory and experimental study.* Miner. Eng. 121, 47–54.

LAPLANTE, A.R., TOGURI, J.M., SMITH, H.W., 1983. *The effect of air flow rate on the kinetics of flotation. Part 1: The transfer of material from the slurry to the froth.* Int. J. Miner. Process. 11(3), 203-219.

LI, H.M., LI, L.X., YANG, X.Q., CHENG, Y.B., 2015. *Types and geological characteristics of iron deposits in China.* J. Asian Earth Sci. 103, 2-22.

LIMA, N.P., VALADAO, G.E.S., PERES, A.E.C., 2013. *Effect of amine and starch dosage on the reverse cationic flotation of an iron ore.* Miner. Eng. 45, 180–184.

LUBISI, T.P., NHETA, W., NTULI, F., 2018. *Optimization of Reverse Cationic Flotation of Low-Grade Iron Oxide from Fluorspar Tails Using Taguchi Method.* Arab J. Sci. Eng. 43, 2403–2412.

LUO, X., WANG, Y., WEN, S., MA, M., SUN, C., YIN, W., MA, Y., 2016. *Effect of carbonate minerals on quartz flotation behavior under conditions of reverse anionic flotation of iron ores.* Int. J. Miner. Process. 152, 1–6.

MA, X., MARQUES, M., GONTIJO, C., 2011. *Comparative studies of reverse cationic/anionic flotation of Vale iron ore.* Int. J. Miner. Process. 100(3–4), 179-183. https://doi.org/10.1016/j.minpro.2011.07.001.

MONTES, S., MONTES-ATENAS, G., 2005. *Hematite floatability mechanism utilizing tetradecylammonium chloride collector*. Miner. Eng. 18, 1032-1036.

Nakhaei, F., Irannajad, M., 2017. *Reagents types in flotation of iron oxide minerals: A review*. Mineral Processing and Extractive Metallurgy Review, 39 (2), 89-124.

PATTANAIK, A., RAYASAM, V., 2018. *Analysis of reverse cationic iron ore fines flotation using RSM-D-optimal design – An approach towards sustainability.* Adv. Powder Technol. 29(12), 3404-3414.

PATTANAIK, A., VENUGOPAL, R., 2018. *Investigation of adsorption mechanism of reagents (surfactants) system and its applicability in iron ore flotation – an overview*. Colloid and Interface Sci. Communications, 25, 41-65.

QUAST, K., 2017. *Literature review on the use of natural products in the flotation of iron oxide ores.* Miner. Eng. 108, 12–24.

RAVISHANKAR, S., KHOSLA, N., 1995. *Selective flocculation of iron oxide from its synthetic mixtures with clays: a comparison of polyacrylic acid and starch polymers.* Int. J. Miner. Process. 43(3–4), 235–247.

Shrimali, K., Atluri, V., Wang, Y., Bacchuwar, S., Wang, X., Miller, J. D., 2018. *The nature of hematite depression with corn starch in the reverse flotation of iron ore*. Journal of Colloidal and Interface Science, 524, 337–349.

SOBHY, A., WU, Z., TAO, D., 2021, *Statistical analysis and optimization of reverse anionic hematite flotation integrated with nanobubbles.* Miner. Eng. 163, 106799.

SOBHY, A., YAHIA, A., EL HOSINY, F.I., IBRAHIM, S.S., AMIN, R., 2019. *Statistical analysis of Egyptian oil shale column flotation.* Int. J. Coal Prep. and Util. https://doi.org/10.1080/19392699.2019.1622530

TANG, Z.D., GAO, P., HAN, Y.X., GUO, W., 2019. *Fluidized bed roasting technology in iron ores dressing in china – a review on equipment development and application prospect*. Journal of Min. and Metall., Section B: Metallurgy, 55 (3)B, 295 - 303.

TAO, D., WU, Z., SOBHY, A., 2021, *Investigation of nanobubble enhanced reverse anionic flotation of hematite and associated mechnaisms.* Powder Technol., 379, 12-25.

WANG, Y., KHOSO, S.A., LUO, X., TIAN, M., 2019. *Understanding the depression mechanism of citric acid in sodium oleate flotation of Ca^{2+}-activated quartz: Experimental and DFT study.* Minerals Engineering, 140, 105878.

WANG, Y., MU, J., WANG, J., 2011, *Optimization of fermentation technology of hawthorn-pear wine by uniform design and response surface design.* Front. Agric. China 5, 407.

WEISSEBORN, P., WARREN, L., DUNN, J., 1995. *Selective flocculation of ultrafine iron ore. 1. Mechanism of adsorption of starch onto hematite.* Colloids Surf., A 99(1), 11–27.

XIA, S., LIN, R., SHAN, J., 2016. *The application of orthogonal test method in the parameters optimization of PEMFC under steady working condition.* Int. J. Hydrogen Energy.

YANG H., TANG Q., WANG C., ZHANG J., 2013. *Flocculation and flotation response of Rhodococcus erythropolis to pure minerals in hematite ores*. Miner. Eng. 45, 67–72.

YANG, S., WANG, L., 2018. *Structural and functional insights into starches as depressant for hematite flotation.* Miner. Eng. 124, 149–157.

YE, H., MATSUOKA, I., 1993. *Reverse flotation of fine quartz from dickite with oleate*. International Journal of Mineral Processing, 40(1-2), 123-136.

YIN, W., FU, Y., YAO, J., YANG, B., CAO, S., SUN, Q., 2017. *Study on the dispersion mechanism of citric acid on chlorite in hematite reverse flotation system*. Minerals 7 (11), 221.

YIN, W., WANG, D., DRELICH, J. W., YANG, B., LI, D., ZHU, Z., YAO, J., 2019. *Reverse flotation separation of hematite from quartz assisted with magnetic seeding aggregation.* Miner. Eng., 105873.

YIN, W.-Z., LI, D., LUO, X.-M., YAO, J., SUN, Q.-Y., 2016. *Effect and mechanism of siderite on reverse flotation of hematite.* Int. J. Miner. Metall. Mater. 23 (4), 373–379.

ZHANG, X., GU, X., HAN, Y., PARRA-ÁLVAREZ, N, CLAREMBOUX, V., 2019. *Flotation of Iron Ores: A Review*. Mineral Processing and Extractive Metallurgy Review, 42(3), 184-212.

ZHANG, Y., HE, Y., ZHANG, T., ZHU, X., FENG, Y., ZHANG, G., BAI, X., 2018. *Application of Falcon centrifuge in the recycling of electrode materials from spent lithium ion batteries*. Journal of Cleaner Prod. doi:10.1016/j.jclepro.2018.08.133